ELSEVIER

Cement and Concrete Composites **19** (1997) 315–328

0958-9465/97/$17.00

PII:S0958-9465(97)00027-9

Tension Softening of Fibre-Reinforced Cementitious Composites

D. Lange-Kornbak[a] & B. L. Karihaloo[b]*

[a]Department of Civil Engineering, University of Sydney, Sydney, NSW 2006, Australia
[b]Institute of Mechanical Engineering, Aalborg University, DK-9220 Aalborg, Denmark

(Received 18 September 1996; accepted 21 May 1997)

Abstract

The complete tension softening behaviour of short-fibre-reinforced cementitious composites which exhibit extensive matrix cracking is established by combining a fracture mechanical approach for bridged, discontinuous cracks with a statistical approach for a bridged, through-crack via consistent relationships for the bridging stress. These relationships account for adhesive and frictional bonding of fibres along a crack and are capable of accommodating the effects of fibre content and pre-peak cracking upon the fibre–binder interfacial properties. The combined approach is adapted to mortars based on a conventional high-strength cement binder and a dense, homogeneous cement–silica binder (DSP composite), and good agreement is obtained between the uniaxial tensile strength so calculated and that based on the rule of mixtures. Although the tension softening model needs many geometrical and mechanical properties of the mix constituents, as well as of the hydration products (e.g. interfaces) and the initial post-peak crack configuration, it provides a powerful tool for microstructural design of fibre-reinforced cementitious composites, particularly DSP mortars. © 1997 Elsevier Science Ltd.

Keywords: Tension softening, fibre reinforced mortars, fracture mechanics, fibre pull-out, fibre bridging stress, uniaxial tensile strength, microsilica, DSP.

INTRODUCTION

Quasi-brittle materials are characterized by the localization of deformation after the attainment of tensile strength, i.e. by the continued opening of cracks and stretching of unbroken material ligaments in a narrow localization zone (band). The overall post-peak stress–inelastic displacement or tension softening response (w,σ) of this zone governs many important structural aspects, such as bearing capacity and brittleness, and has accordingly received considerable attention in a number of studies. Within the framework of fracture mechanics, the tension softening response has been established by modelling the localization zone as a series of unbridged[1–5] (i.e. traction-free) or bridged cracks.[6]

In unreinforced cementitious composites, the partial bridging provided by unbroken material ligaments (typically aggregates) in the fracture process zone near the crack tips may be accounted for by considering Dugdale-type cracks[1,7,8] or a bridged effective through crack.[9] Alternatively, an appropriate value can be assigned to the fracture toughness of the material.[4,10] Moreover, after coalescence of the cracks, the pull-out of large aggregates along the through crack can be considered, as suggested by Huang & Li.[4]

For discontinuous fibre-reinforced cementitious composites, Karihaloo *et al.*[6] assumed the fragmented cracks to be bridged along their entire length, the continuous closing pressure being obtained by smearing the discrete closing forces provided by the fibres. However, the tension softening response was only studied prior

* Present address: University of Wales Cardiff, School of Engineering, Cardiff CF2 1XH, UK.

to coalescence of the cracks, although the fibres usually continue to bridge after the formation of a through crack[11] (Fig. 1). The multiple-crack model of Karihaloo *et al.*[6] and the through-crack model of Li *et al.*[11] are appropriately combined in the following to yield the complete tension softening behaviour of fibre-reinforced cementitious composites. The cracks in both models are bridged, the bridging being provided entirely by fibres. Thus, the cracks are assumed to traverse exclusively through the matrix and not through the aggregate particles or along aggregate–matrix interfaces. This type of crack configuration is characteristic of mortars using cement, silica, and strong aggregates.

In the present study, particular emphasis is placed on mortars based on the DSP (densified systems containing homogeneously arranged ultra-fine particles) concept,[12] which, contrary to conventional mortars, are highly homogeneous, thereby enabling a high degree of packing. The homogeneity is achieved by effectively eliminating (reducing) the surface forces responsible for the flocculation of the particles in the fresh binder primarily through the use of surface-active agents. The high strength of the binder thus produced reduces the resistance to microcracking induced during hydration and increases the brittleness of the composite using this binder as matrix. This may be remedied through various particle (aggregate and fibre) modifications. The densely packed cement particles, partly dissolved in sufficient water to ensure water saturation, are responsible for part of the strength gain due to a high density of chemical and physical bonds and due to the toughening (crack deflection and bridging) generated by the unhydrated parts of the cement particles. In addition, the ultrafine microsilica particles in the voids between the cement particles reduce the amount of water required for water saturation, thereby further enhancing the strength as the porosity and pore size distribution are improved.[13] Moreover, the density and strength of bonds increase (partly due to the replacement of weak calcium hydroxide by strong calcium silicate hydrate through the pozzolanic reaction of microsilica) and the undissolved microsilica provides additional toughening. The reduction in water demand (and the associated reduction in the amount of cement paste), together with the restraining action of the stiff, partly undissolved microsilica, reduces the overall inherent (autogeneous) shrinkage of the cement–silica binder. At the same time, however, the fine and dense microstructure produces large contractive forces[12] such that the shrinkage action approaches (or exceeds[14]) that of ordinary cement paste. Nonetheless, because of the substantially improved strength, the resistance to microcracking is lowered, i.e. the brittleness number[15] $B = [g(f'_{t,matrix})^2]/(E_{matrix} G_{F,matrix})$ is increased. Here, g is the maximum size (diameter) of the aggregate particles in a matrix with uniaxial tensile strength $f'_{t,matrix}$, and E_{matrix} and $G_{F,matrix}$ are Young's modulus and specific fracture energy of matrix. For structural purposes it is essential to reduce the content of shrinking binder by incorporating a high volume fraction

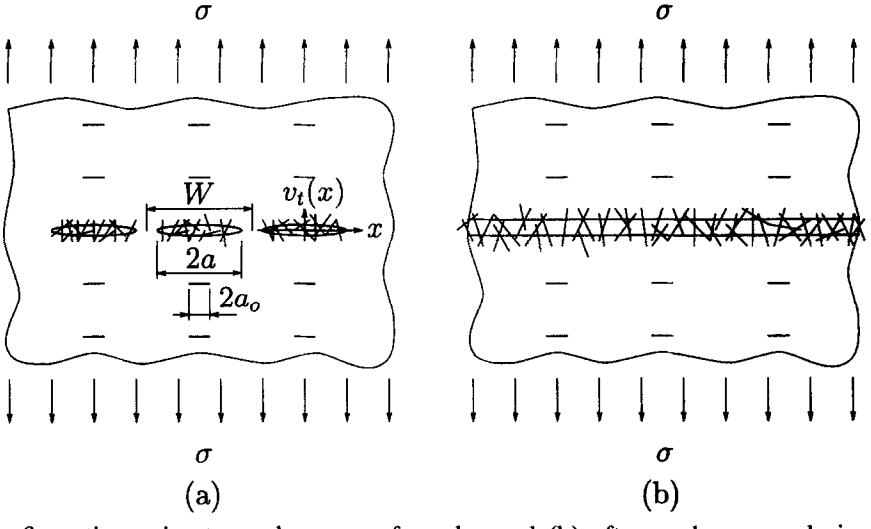

Fig. 1. (a) Crack configuration prior to coalescence of cracks, and (b) after coalescence, during tension softening of fibre-reinforced quasi-brittle materials.

of small aggregate particles to avoid a deterioration in B. Whereas this only marginally improves B, substantial improvement is achieved by incorporating fibres which primarily increase $G_{F,matrix}$.

Aggregate–matrix interfacial cracks (often leading to a coherent crack pattern) can be avoided, or at least reduced, by using rough aggregate particles, such as calcined bauxite.[16]

TENSION SOFTENING MODEL

The model is based on effective cracks approximating the mechanical behaviour of the physical 'crack' (Fig. 2(a)). The physical crack is initially a collection of small unbridged cracks (including Cook–Gordon interfacial cracks) which eventually connect and perhaps propagate along the matrix–fibre interface (herein referred to as peeling — not to be confused with slip) depending on its brittleness. Crack opening due to rupture (which may be avoided if the fibres are sufficiently short) and peeling of the fibres will be assumed to be negligible, such that inelastic opening is produced only when the fibres lose their adhesive bond to the matrix and slip under establishment of frictional bonding in a zone of length $2b$. $v_t(x)$ denotes the local half-opening of the effective crack.

The distribution of bridging stress along the effective crack $p(v_t)$ is taken to conform with the slip-weakening behaviour exhibited by steel fibres,[17] see Fig. 2(b). For this purpose, a tri-

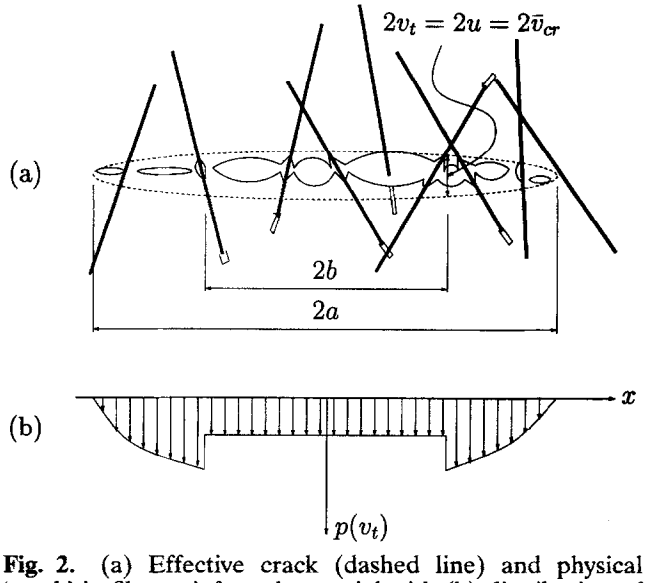

Fig. 2. (a) Effective crack (dashed line) and physical 'crack' in fibre-reinforced material with (b) distribution of bridging stress $p(v_t)$ prior to coalescence of cracks.

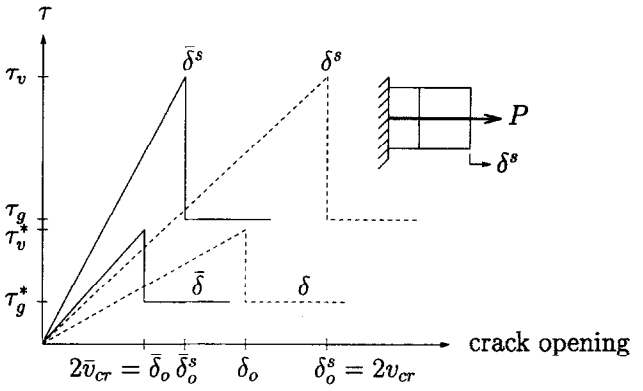

Fig. 3. Idealized interfacial matrix–fibre shear stress (τ) vs. crack mouth opening (elongation of fibre) (δ) or effective crack opening ($\bar{\delta}$) relationship for single-fibre (superscript s) and multiple-fibre pull-out.

linear idealization of the interfacial shear stress–crack opening relationship is adopted (Fig. 3). As indicated, this relationship depends on the volume fraction of fibre present in the pull-out test specimen[17,18] and it may be expressed in terms of the mouth opening of an artificial crack (identical to the elongation of fibre) δ, or an equivalent measure of the crack opening, e.g. that of the effective crack, $\bar{\delta} = 2v_t$. The latter is desirable in the present study as the multiple-crack model provides values of v_t. τ_v (τ_v^*) is the adhesive bond strength, τ_g (τ_g^*) the frictional bond strength and δ^s (δ) the elongation of the fibre (or crack mouth opening) in a single-fibre (multiple-fibre) pull-out test. Furthermore, δ_0^s and δ_0 are the respective crack mouth openings at initiation of fibre pull-out, whereas $\bar{\delta}^s$, $\bar{\delta}_0^s$, $\bar{\delta}$ and $\bar{\delta}_0$ denote corresponding effective crack openings.

The tri-linear relationship enables establishment of simple expressions for the bridging force provided by a fibre $P(\bar{\delta})$ *or* $P(\delta)$. Li *et al.*[11] suggested a relation between $P(\delta)$ and the bridging stress $p(\delta)$ by considering frictionally bonded fibres along a through crack. Applying this relationship to adhesively bonded fibres and multiple effective cracks, it reads

$$p(\bar{\delta}) = \frac{V_f}{A_f} \int_{\phi=0}^{\pi/2} \int_{z=0}^{(L/2-\bar{\delta})\cos\phi} P(\bar{\delta},\phi,z)p(\phi)p(z)\,dz\,d\phi \qquad (1)$$

where V_f is the volume fraction of fibre, A_f the cross-sectional area of a fibre, L the initial length of a fibre, ϕ the orientation angle of the fibre to a plane perpendicular to the crack and z the distance from the centroid of the fibre to

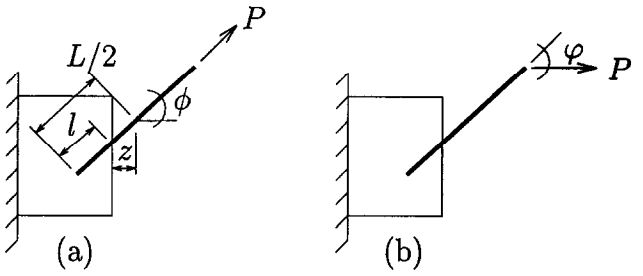

Fig. 4. (a) Single-fibre pull-out without snubbing ($\varphi = 0$) and (b) with snubbing ($\varphi \neq 0$, $\phi = \varphi$).

the crack plane, see Fig. 4. The probability densities are $p(\phi) = \sin\phi$ and $p(z) = 2/L$. Moreover, to account for the snubbing effect (fibre dowel action) arising when a fibre is not loaded in the direction of the initial straight fibre (Fig. 4), the bridging force is increased according to $P(\bar{\delta},\phi = \varphi,l) = P(\bar{\delta},\phi,\varphi = 0,l)\, e^{f\phi}$, where φ is the orientation angle of the fibre to the loading direction and f the snubbing friction coefficient.

Motivated by similar models, the bridging stress for multiple-fibre bridging will be expressed in terms of single-fibre properties τ_v and τ_g. This is achieved by introducing the ratio

$$\zeta = \frac{\bar{\delta}_0}{\delta_0^s} = \frac{\bar{v}_{cr}}{v_{cr}} \tag{2}$$

where $\bar{v}_{cr}$ follows from the multiple-crack model, since it assumes slippage to be initiated immediately after reaching the ultimate tensile load, whereby the corresponding maximum half-opening of the crack equals $\bar{v}_{cr}$. (This type of slippage behaviour is in accord with the work of Tjiptobroto & Hansen[19] for DSP composites.) v_{cr} may be estimated by considering the onset of slip of a single fibre (with diameter d) bridging perpendicularly an initially closed crack that separates the material parts shown in Fig. 5(b). A similar pull-out test set-up has been employed by e.g. Banthia & Yan.[20] The estimate will be based on a stress (strength) approach; more refined fracture mechanics (energy-based) approaches are also available.[18,21,22] (The so-called mismatch-strain approach is also available.[23]) Near the crack mouth, the opening will attain a constant value, δ_0^s, equal to the displacement of the load point. As the fibre undergoes the same amount of deformation, it will experience an average strain of δ_0^s/L and a strain of $2\delta_0^s/L$ across the crack provided peeling is limited. The bridging stress is $P_0/(\pi d^2/4)$ with $P_0 = \tau_g' \pi d l' = \tau_g \pi d l$ — the bridging force carried by the fibre at the attainment of slip over the entire embedded length l'. Owing to peeling, the short embedded fibre segment is reduced from l to l'. For a linear-elastic fibre, therefore, the critical half-crack opening at onset of full slippage becomes $v_{cr} = 1/2\ \delta_0^s = (\tau_g L l)/(E_f d)$. Similar expressions have been reported by Li,[24] Li *et al.*,[25] and Balaguru & Shah.[18] The interfacial shear stress prior to slippage is given by $\tau = \bar{\delta}\tau_v^*/(\delta_0^s\zeta)$, resulting in $P = (\tau_v^*/\zeta)[E_f d^2\pi/(2\tau_g L)]\, e^{f\phi}\bar{\delta}$, while during slippage $P = \tau_g^* \pi d l[1-(\bar{\delta}-\bar{\delta}_0)/l]\, e^{f\phi}$. In performing the integrations indicated in eqn 1, it is assumed that ζ attains its mathematical expectation $E(\zeta) = \bar{v}_{cr}/E(v_{cr})$, where

$$E(v_{cr}) = \frac{\tau_g L}{E_f d} E(l) = \frac{\tau_g L}{E_f d}\left[\frac{L}{2} - \frac{E(z)}{\cos\phi}\right]$$

$$= \frac{1}{4}\frac{\tau_g L^2}{E_f d} \tag{3}$$

following the observation by Li *et al.*[11] that $l = L/2 - z/\cos\phi$ has a distribution according to

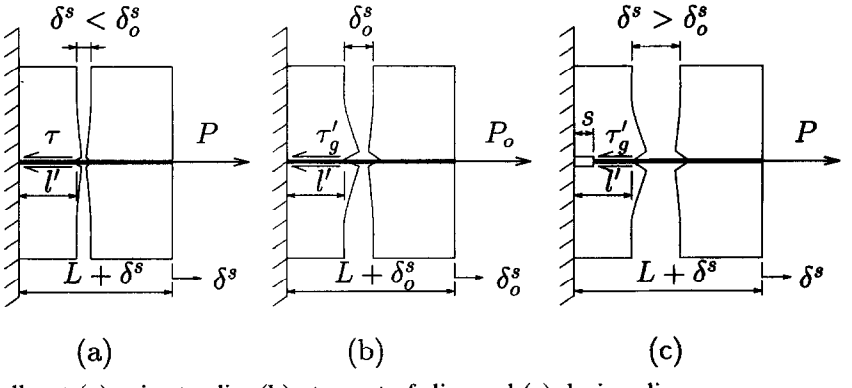

Fig. 5. Single-fibre pull-out (a) prior to slip, (b) at onset of slip, and (c) during slip.

the probability densities of ϕ and z. Further, making use of the observation[17] $\tau_v^*/\bar{v}_{cr} \approx \tau_v/v_{cr}$ and the assumption $\tau_g^*/\bar{v}_{cr} \approx \tau_g/v_{cr}$, we eventually have (see Appendix A for details)

$$p(v_t) = \begin{cases} 2V_f \dfrac{\tau_v}{\tau_g} E_f h \left(\dfrac{1}{L} v_t - \dfrac{4}{L^2} v_t^2 \right) \approx 2V_f \dfrac{\tau_v}{\tau_g} E_f \dfrac{h}{L} v_t, & v_t < \bar{v}_{cr} \\ V_f \tau_g \dfrac{L}{d} \dfrac{1}{2} hE(\zeta) \left[-2 \left(\dfrac{2v_t}{L/2} \right) + (2-\alpha) \left(\dfrac{2v_t}{L/2} \right)^2 + \alpha \right] \approx V_f \tau_g \dfrac{L}{d} \dfrac{1}{2} h\zeta, & v_t \geq \bar{v}_{cr} \end{cases} \quad (4)$$

Here, the snubbing factor $h = 2/(4+f^2)(e^{f\pi/2}+1)$ and $\alpha = 1+\{[2\tau_g LE(\zeta)]/(E_f d)\}(\approx 1)$. The exact $p(v_t)$ expression for $v_t \geq \bar{v}_{cr}$ is identical to Li's[24] tension softening relation $p(\delta)$ when $\alpha = 1$ and $\bar{\delta} = 2v_t \approx \delta$ for large crack openings. It should be clear, however, that $\bar{\delta}$ is not the sought inelastic crack opening w but rather the elastic $(\bar{\delta}_0)$+inelastic crack opening (w) such that the tension softening relation after the through crack has formed at $w = w_k$ becomes

$$\sigma(w) = \sigma(\bar{\delta} - \bar{\delta}_0) = V_f \tau_g \zeta \frac{L}{d} \frac{1}{2} \times h \left[-\frac{4}{L} w + \frac{4}{L^2} (2-\alpha) w^2 + \alpha \right], \quad w > w_k \quad (5)$$

with $\sigma(w) = 0$ for $w = (L/2)[1-\sqrt{1-\alpha(2-\alpha)}]$ $(= L/2$, the largest fibre embedment length, for $\alpha = 1)$.

We finally turn our attention to the tension softening response prior to coalescence of the cracks, i.e. $w \leq w_k$. For a given crack configuration (a,b,W) and applied stress σ the model by Karihaloo *et al.*[6] provides the corresponding stress intensity factor K_I and crack openings v_t. In particular, at peak load $(\sigma = f_t', a = a_0, b = 0)$, we determine the fracture toughness $K_{Ic} = K_I$ and $\bar{v}_{cr}$. For $K_I = K_{Ic}$ in the entire post-peak regime, the model predicts a decreasing w when the crack propagates beyond a certain crack length. In reality, however, w increases monotonically. For an ideal brittle material this is believed to be accomplished by the deviation of the cracks from their plane[26], whereby K_I decreases below the value predicted by the original model, whereas for quasi-brittle materials, such as those studied herein, the resistance to crack propagation K_{Ic} is enhanced presumably by the interaction of the process zones. The increase in K_{Ic} is manifested through a change in sign of the curvature $\partial^2\sigma/\partial w^2$ of (σ,w) diagram at $a > a_i$ (corresponding to points of instability). Thus, for $a > a_i$, K_{Ic} is increased ($K_{Ic} = 0.01$ MPa $m^{0.5}$) such that instability is avoided, i.e. $\partial^2\sigma/\partial w^2$ maintains the same sign throughout tension softening. It is found, however, that this condition can no longer be satisfied when the cracks are very close to one another, i.e. when $a > a_c$. At $a = a_c$, only a few fibres along the discontinuous crack segments remain elastically bonded to the matrix. Hence, an instantaneous drop in the stress is to be anticipated (similar to the pull-out of single fibres, see Fig. 3) when the crack fragments link up to form a through crack. Ortiz[2], amongst others, claims that a sudden drop is inevitable even without fibres when the discontinuous crack fragments link up to form a through crack.

The tension softening relation, i.e. the inelastic deformation of the localization zone, is given by

$$w(\sigma) = \frac{2}{W} \left[\int_{-a}^{a} v_t(\sigma,x)\, dx - \int_{a_0}^{a_0} v_t(f_t',x)\, dx \right] \quad (6)$$

as the opening of the cracks prior to the attainment of peak load is assumed to be purely elastic and the additional opening after the attainment of peak load is assumed to be purely inelastic. For a given half-length of crack a, w corresponds to the values of the unknown stress and of the sliding zone b at which the following two conditions for crack growth are simultaneously satisfied

$$K_I(\sigma,a;b) = K_{Ic}(a_0,W,\tau_v,\tau_g,V_f,f,L,d,E_f,E,f_t') \quad (7)$$

$$u(\sigma,a;b) = \bar{v}_{cr}(a_0,W,\tau_v,\tau_g,V_f,f,L,d,E_f,E,f_t') \quad (8)$$

Here $u(\sigma,a;b)$ is the total crack opening at the ends of the assumed sliding zone.

Nielsen[27] has shown that the modulus of elasticity of a two-phase isotropic composite is given by

$$E = E_m \frac{n+\Theta+V\Theta(n-1)}{n+\Theta-V(n-1)} \quad (9)$$

where V is the volume fraction of the discrete phase, Θ is a geometry function accounting for the configuration of the discrete phase and n is the ratio of the modulus of elasticity of the discrete phase to the modulus of elasticity of the continuous phase E_m. Cement paste, mortar and concrete can be regarded as two-phase composites with the modulus of elasticity given by[28] eqn 9. For cement paste ($E = E_p$), a distinction is made between water/cement ratios below and above 1.2 ρ_w/ρ_c (ρ_w is the density of water; ρ_c is the density of unhydrated cement particles). In the former range, the cement paste is considered as a collection of unhydrated cement particles with modulus of elasticity E_u embedded in partially hydrated cement gel with $E_m = 27200h$ MPa, where h is taken as the relative degree of hydration. The volume fraction of unhydrated cement particles is

$$V = \frac{1-0.83h(w/c)(\rho_c/\rho_w)}{1+(w/c)(\rho_c/\rho_w)} \quad (10)$$

and

$$\Theta = 0.5[\eta_u\sqrt{1-V}(1-n)+\sqrt{\eta_u^2(1-V)(1-n)^2+4n}] \quad (11)$$

where η_u is a shape factor of an unhydrated cement particle. For $w/c > 1.2\rho_w/\rho_c$, the cement paste is regarded as a collection of capillary pores embedded in solid, hydrated cement gel. Now, $n = 0$, $\Theta = \eta_k(1-V)$ with η_k being a shape factor of a capillary pore and the volume fraction of capillary pores

$$V = \frac{w/c-1.2h\rho_w/\rho_c}{w/c+\rho_w/\rho_c} \quad (12)$$

For mortar ($E = E_r$), $E_m = E_p$, n is the ratio of modulus of elasticity of the fine aggregate particles E_s to E_p and $V = V_s$. Moreover,[29]

$$\Theta = \frac{1}{2}\{q+\sqrt{q^2+4n[1-\eta_s(1-V_s)-\eta_s(V_s-1)]}\} \quad (13)$$

Here, $q = \eta_s(1-V_s)+n\eta_s(V_f-1)$ and

$$\eta_s = \frac{3A_s(1+A_s)}{1+A_s+4A_s^2} \quad (14)$$

with A_s being the aspect ratio of the fine aggregate particles. Having determined the modulus of elasticity of the matrix phase in a fibre-reinforced composite from the expressions in eqn 9–14, eqn 9 can again be used to find E of the fibre composite. Now, let $V_f = V$ and[30]

$$\Theta = \frac{1}{2}[\mu+n\mu'+\sqrt{(\mu+n\mu')^2+4n(1-\mu-\mu')}] \quad (15)$$

in which

$$\mu = \mu_0\frac{c_d-V_f}{c_d}$$

$$\mu' = min\left(\mu_0\frac{V_f-c_D}{c_d},1\right)$$

$$\mu_0 = \frac{3A(1+A)}{1+A+4A^2}$$

$$c_d = \frac{\mu_0}{1+\mu_0}$$

$$c_D = \frac{(2c_d)^{10}}{2} \quad (16)$$

and the aspect ratio $A = L/d$ and $n = E_f/E_b$.

The uniaxial tensile strength of the fibre composite follows from

$$f_t' = \frac{P_f+P_b}{W^2} \quad (17)$$

where the contributions from the fibres and the remaining material are respectively

$$P_f = p(v_t = w_t/2)W^2 = V_f\frac{\tau_v}{\tau_g}E_f\frac{h}{L}w_t(\sigma = f_t')W^2$$

(18)

$$P_b = f'_{t,b}(1-V_f)(W^2-4a_0^2) \quad (19)$$

The total effective deformation of the localization zone is

$$w_t(\sigma) = \frac{w_{lig}(W-2a)}{W} + \frac{2}{W}\int_{-a}^{a} v_t(\sigma,x)\,dx \quad (20)$$

In the unbroken ligaments, strain compatibility between the matrix and the fibres is assumed, such that $w_{lig} = f'_{t,b}L/E_b$. The uniaxial tensile strength for a particulate composite as established by Huang & Li[4] yields

$$f'_{t,b} = \frac{K_{Ic,p}}{\sqrt{\pi g/2}}\,\eta$$

where η is the toughening ratio due to various toughening mechanisms, $K_{Ic,p}$ is the fracture toughness of the binder and g is the maximum aggregate size (diameter). For a material with a strong aggregate–matrix interface and small, strong aggregate particles with tensile strength $f'_{t,a}$ and average size (diameter) g_{av} the toughening may be assumed to be caused by crack deflection, bridging and trapping, whereby[4,31]

$$\eta = \sqrt{1.0+0.87V} \times$$

$$\sqrt{\chi^2 + \frac{E'_b(\pi/2)f_{t,a}^2 g_{av} V(1-\sqrt{V})(1-V)(1-\nu_p^2)}{E_b(1-\nu^2)(K_{Ic,p})^2}} \quad (22)$$

where

$$\chi = \left(1 - \frac{(1-V)\pi/4}{ln\{[1+cos(\pi V/2)]/sin(\pi V/2)\}}\right)^{-1}$$

$$\frac{E'_b}{E_b} = 1 - \frac{\pi^2}{16}(1-\nu^2)V$$

E'_b is the modulus of elasticity of the composite exclusive of the fibres with interfacial cracks, whereas E_b is that without interfacial cracks. V is the volume fraction of aggregates. For the cement binder, Lange-Kornbak & Karihaloo[32] proposed the empirical relation between $K_{Ic,p}$ and water to cement (w/c) ratio

$$K_{Ic,p} = 0.6125 - 0.85 w/c \text{ MPa m}^{0.5} \quad (23)$$

for $0.2 \le w/c \le 0.45$.

Table 1. Values of microstructural parameters for selected mortars

Microstructural parameter	Mix I	Mix II
V_c	0.4741	0.4741
V_{ms}	0.1627	0
V_f	variable	variable
g (mm)	4.0	4.0
g_{av} (mm)	1.0	1.0
a_0 (mm)	variable	variable
W (mm)	50.0	50.0
$f'_{t,a}$ (MPa)	10.0	10.0
E_a (MPa)	65000	65000
E_f (GPa)[33]	210.0	210.0
L (mm)	20	20
d (mm)	0.4	0.4
τ_v (MPa)[12,18,21]	9.0	3.0
τ_g (MPa)[12,18,21]	5.0	2.5
f[1,24]	0.9	0.75

DISCUSSION

In the following, two mixes with the microstructural parameters given in Table 1 are compared. Mix I is a cement–silica-based DSP binder, whereas mix II is based on a conventional high-strength cement binder. Both mixes contain round, plain straight steel fibres. The composition of the binder follows from $1 = V_{ms}+V_c+V_w$ with V_{ms} the volume fraction (packing density) of microsilica particles, V_c that of cement particles and V_w that of water (and dispersing agent). The volume fraction of fine aggregate is given by $(1-V_p-V_f)/(1-V_f)$ where the volume fraction of paste is $V_p = 0.5$ for all V_f used in the tests by Tjiptobroto & Hansen.[19] Note that $w/c = V_w\rho_w/(V_c\rho_c)$. It is assumed that $K_{Ic,p} = 0.5$ MPa m$^{0.5}$ and $E_p = 35000$ MPa for mix I and that crack trapping is absent (i.e. $\chi = 1.0$) in mix II. The study of Tjiptobroto & Hansen[19] suggests that the crack spacing W is only marginally affected by the variation in paste composition studied here. Following the work of Karihaloo *et al.*[6] $W = 50$ mm is chosen for both mixes. Moreover, any alteration in W due to a variation in V_f has been neglected.

A comparison of eqn 17 with the rule of mixtures[18,21]

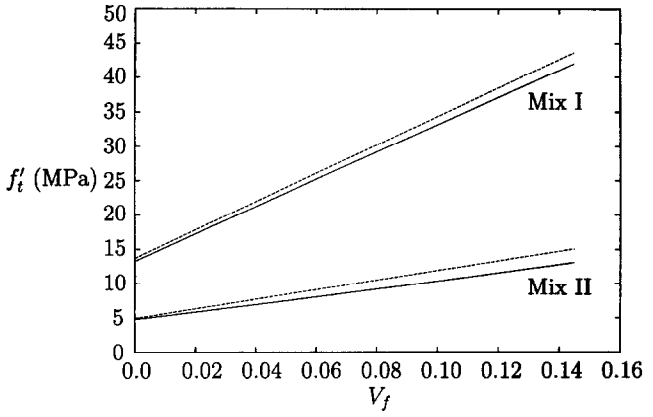

Fig. 6. Uniaxial tensile strength as a function of volume fraction of fibre according to eqn 17 (solid line) and eqn 24 (dashed line) ($a_0 = 4.5$ mm).

$$f_t' = \gamma f_{t,b}'(1 - V_f) + \beta \tau_v V_f \frac{L}{d} \qquad (24)$$

appears to lend considerable support to the proposed model, as good agreement is obtained for both mixes in the entire range of V_f values, see Fig. 6. In the comparison $\gamma = 1$, so that $f_t' = f_{t,b}'$ at $V_f = 0$, and $\beta = 0.5$ are in agreement with the use of randomly distributed short fibres.[6] The rise in f_t' with an increase in V_f is predominantly an effect of V_f as $f_{t,b}'$ and $\bar{v}_{cr}$ (see Fig. 7) are found to be only marginally influenced by this parameter; $f_{t,b}'$ varies from 4.95 MPa (13.69 MPa) at $V_f = 0$ to 4.87 MPa (12.85 MPa) at $V_f = 0.145$ for Mix I (II). For practical conventional mixes, the homogeneity of the paste and the random distribution of fibres cannot be maintained at more than a few percent fibres so that the increase in f_t' is less pronounced than shown in Fig. 6; even a decrease in f_t' may be experienced. In other words, at increasing V_f the numerical coefficients γ and β in eqn 24 are reduced. In the proposed theoretical model, however, $K_{Ic,p}$, τ_v and τ_g would decrease with increasing V_f and the probability densities $p(\phi)$ and $p(z)$ in eqn 1 would change according to the actual statistical distribution of the fibres. For DSP mixes, on the other hand, measurements of the flexural tensile strength, compressive strength and specific fracture energy indicate that the homogeneity of the paste and the random distribution of fibres is maintained up to at least[19,34] $V_f = 0.12$.

The loss in strength resulting from increased crack length a_0 shown in Fig. 8 can be attributed to the reduction in P_b, which is only partly compensated by an increase in P_f ($\bar{v}_{cr}$) at small a_0 (Fig. 9). The variation of $\bar{v}_{cr}$ with a_0 noticeable in Fig. 9 results from the averaging implied in eqn 20.

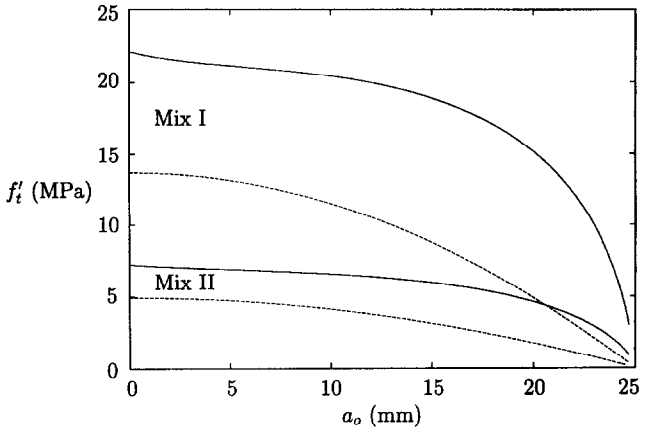

Fig. 8. Variation of uniaxial tensile strength with half-length of crack a_0 at ultimate tensile load for bridged ($V_f = 0.04$, solid line) and unbridged cracks ($V_f = 0$, dashed line).

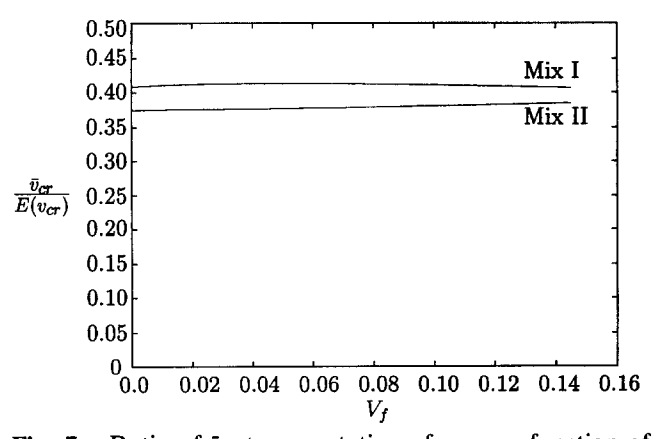

Fig. 7. Ratio of $\bar{v}_{cr}$ to expectation of v_{cr} as a function of volume fraction of fibre ($a_0 = 4.5$ mm).

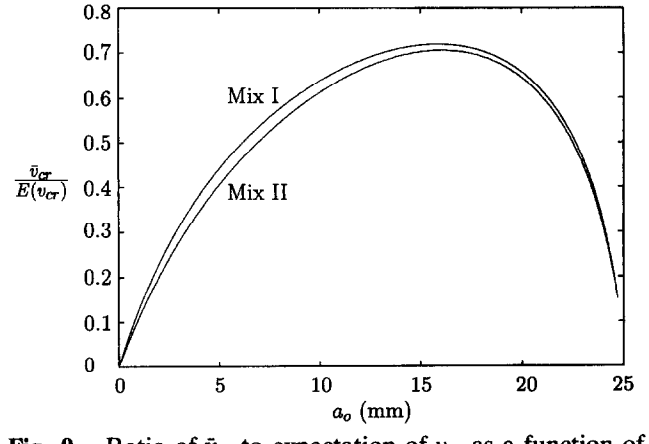

Fig. 9. Ratio of $\bar{v}_{cr}$ to expectation of v_{cr} as a function of half-length of crack a_0 at ultimate tensile load ($V_f = 0.04$).

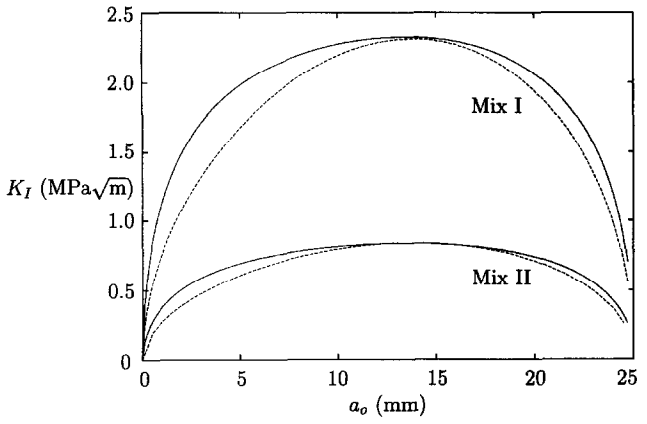

Fig. 10. Variation of stress intensity factor K_I with half-length of crack a_0 at ultimate tensile load for bridged ($V_f = 0.04$, solid line) and unbridged cracks ($V_f = 0$, dashed line).

Further support to the model is provided in Fig. 10, which shows that the variation of K_I in the post-peak regime (where $K_I = K_{Ic}$) with a_0 follows the trend established for unbridged cracks. In the latter case,[35] $K_I = K_{Ic} = \sqrt{W \tan(\pi a_0/W)} f_t'$. As expected, K_I (K_{Ic}) is the greatest for the densest mix and the largest V_f. At large a_0, the reduction in K_{Ic} caused by the lower f_t' and bridging stress (see Fig. 9) overshadows the enhancement arising from increases in a_0.

Figure 11 shows the bridging stress–total crack opening relationship according to eqn 4. For other values of the half-length of crack a_0 at peak load, the modified relationship follows from the value of $E(\zeta)$ as $\bar{v}_{cr}$, unlike v_{cr}, is affected by a_0. With $\bar{v}_{cr} = E(v_{cr})E(\zeta)$, the maximum and the residual bridging stress follow from eqn 4. Figure 9 shows that the bridging stresses increase with increasing a_0 up to about 16 mm, so that the fibres provide the most efficient bridging as expressed by $E(\zeta)$, when medium-sized cracks are present at ultimate load. The same figure provides the crack opening $\bar{v}_{cr}$ required for crack propagation at a given crack length. It also reflects the assumption that fibre pull-out is initiated at the onset of tension softening where the maximum crack opening is $\bar{v}_{cr}$ and not on the descending branch when the maximum crack opening reaches v_{cr}. a_0 is controlled by the brittleness of the binder and V_f; a higher brittleness and lower content of fibre result in larger crack lengths (a_0). However, Fig. 9 does not take into account that τ_g ($E(v_{cr})$) is affected by the brittleness (composition) of the binder associated with variations in a_0.

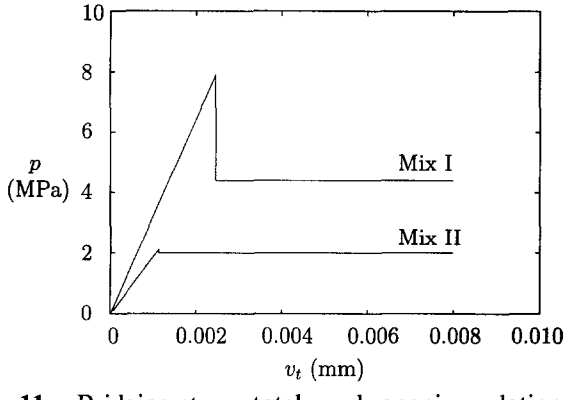

Fig. 11. Bridging stress–total crack opening relationship ($a_0 = 4.5$ mm).

The tension softening responses are shown in Fig. 12. For Mix I (II), K_{Ic} has increased from 1.93 MPa m$^{0.5}$ (0.67 MPa m$^{0.5}$) at $a_i = 0.0185$ mm (0.0195 mm) to 6.09 MPa m$^{0.5}$ (2.21 MPa m$^{0.5}$) at $a_c = 0.02493$ mm. It is noted that the fracture energy G_F of the fibre-reinforced DSP material is 16000 Nm/m^2, which is within the range 5000–40000 Nm/m^2 reported for these materials.[34]

Two aspects of the above calculations need to be stressed. First, there are 32 integration points per half-crack length. As the bridging zone is restricted to grow discontinuously from one integration point to the next, K_I and u are allowed to deviate 5% from the target values (K_{Ic} and $\bar{v}_{cr}$ respectively) in order to be able to satisfy the crack growth criteria in eqns 7–8. Secondly, a unique tension-softening curve is determined by letting the stress to decrease, i.e. letting a increase from a_0, as the snap-back (instability) in the tail region predicted by the

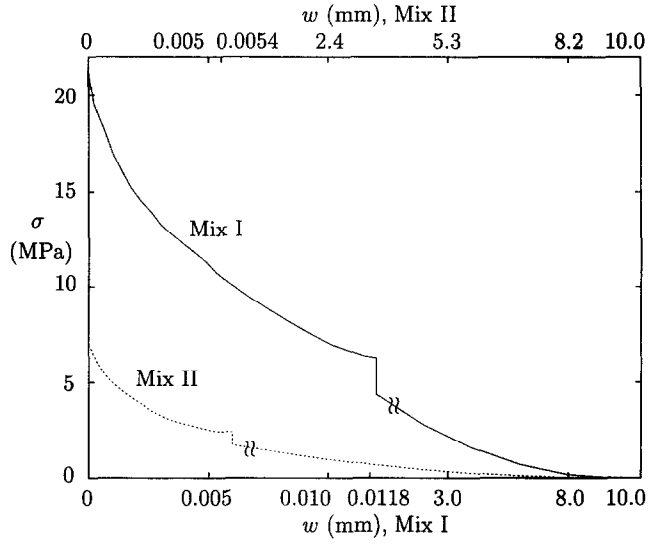

Fig. 12. Tension softening response.

original model represents a series of bifurcation points that can lead to different tension-softening curves when the stress is increased, i.e. a is decreased towards a_0.

CONCLUSIONS

The present study has established the complete tension softening response of short-fibre-reinforced cementitious composites in which the cracks in the localization zone are bridged along their entire length by adhesively or frictionally bonded fibres. This is achieved by using a consistent bridging-stress relationship in two existing models. The first model, suggested by Karihaloo *et al.*,[6] is applicable to the initial growth of discontinuous crack segments, whereas the other model by Li *et al.*[11] describes the tension softening behaviour after coalescence of the cracks into a through crack. The former model is additionally modified by imposing a stability criterion on crack growth which involves an increase in fracture toughness immediately before the cracks link up to form a through crack.

Besides giving the specific fracture energy G_F of the composite, the proposed model is capable of predicting the uniaxial tensile strength f_t' which is in good agreement with the rule of mixtures. Nonetheless, the assumption that fibre pull-out is initiated at onset of tension softening needs verification. Further improvement of the model is possible by a more accurate prediction of the initial post-peak crack configuration.

Having established the relationships between the effective properties (i.e. direct tensile strength f_t', fracture energy G_F and modulus of elasticity E) of a fibre-reinforced concrete mix and its microstructural parameters (e.g. fibre–matrix interfacial adhesive or frictional bond strength, length of fibres, diameter of fibres, volume fraction of fibre and volume fraction of aggregates) it is possible to design such composites for simultaneous minimum brittleness, i.e. maximum characteristic length $EG_F/f_t'^2$, and maximum tensile strength. This can be accomplished with the use of mathematical programming techniques, as demonstrated for plain concrete.[32] The results for short-fibre-reinforced cementitious composites based on the DSP concept will be reported in a future communication.

ACKNOWLEDGEMENTS

The authors would like to acknowledge Dr. Jianxiang Wang's assistance with numerical computations.

REFERENCES

1. Horii, H., Hasegawa, A. & Nishino, F., Fracture process and bridging zone model and influencing factors in fracture of concrete. In Proc. SEM-RILEM Int. Conf. 1987, *Fracture of Concrete and Rock*, eds S. P. Shah & S. E. Swartz, Springer-Verlag, New York, 1989, pp. 205–219.
2. Ortiz, M., Microcrack coalescence and macroscopic crack growth initiation in brittle solids. *Int. J. Solids Struct.*, **24**(3), (1988) 231–250.
3. Huang, X. & Karihaloo, B. L., Tension softening of quasi-brittle materials modelled by singly and doubly periodic arrays of coplanar penny-shaped cracks. *Mech. Mater.*, **13** (1992) 257–275.
4. Huang, J. & Li, V. C., A meso-mechanical model of the tensile behaviour of concrete. Part II: modelling of post-peak tension softening behaviour. *Composites*, **20**(4), (1989) 370–378.
5. Karihaloo, B. L., Fu, D. & Huang, X., Modelling of tension softening in quasi-brittle materials by an array of circular holes with edge cracks. *Mech. Mater.*, **11** (1991) 123–134.
6. Karihaloo, B. L., Wang, J. & Grzybowski, M., Doubly periodic arrays of bridged cracks and short fibre reinforced cementitious composites. *J. Mech. Phys. Solids*, **44** 10 (1996) 1565–1586.
7. Shum, D. K. M., Analysis of stable crack growth in brittle materials. Part I: a process zone model. *Int. J. Fract.*, **75** (1996) 95–114.
8. Shum, D. K. M., Analysis of stable crack growth in brittle materials. Part II: a bridge zone model. *Int. J. Fract.*, **75** (1996) 115–136.
9. Stang, H., Evaluation of properties of cementitious materials. In Proc. RILEM/ACI Int. Workshop 1992, *High Performance Fiber Reinforced Cement Composites*, eds H. W. Reinhardt & A. E. Naaman. E.&F.N. Spon, London, 1992, pp. 388–406.
10. Karihaloo, B. L., Tensile response of quasi-brittle materials. In Proc. RILEM-ESIS Int. Conf. 1991, *Fracture Processes in Concrete, Rock and Ceramics*, eds J. G. M. van Mier, J. G. Rots & A. Bakker. E.&F.N. Spon, London, 1991, pp. 163–172.
11. Li, V. C., Wang, Y. & Backer, S., A micromechanical model of tension-softening and bridging toughening of short random fibre reinforced brittle matrix composites. *J. Mech. Phys. Solids*, **39** 5 (1991) 607–625.
12. Bache, H. H., Densified cement/ultra-fine particle-based materials. CBL Report no. 40. Aalborg Portland, Denmark, 1981.
13. Hjorth, L., Development and application of high-density cement-based materials. *Philos. Trans. R. Soc. London Ser. A:*, **310** (1983) 167–173.
14. Jensen, O. M., Autogen deformation og RF-ændring — selvudtørring og selv-udtørringssvind. Report TR-284. Technical University of Denmark, 1993 (in Danish).
15. Bache, H. H., Durability of concrete — fracture mechanical aspects. *Nordic Conc. Res.*, **4** (1985) 7–25.
16. Lange-Kornbak, D., Concrete microcracking — effect of aggregate geometry. M.Sc. Thesis. Dept. of Build-

ing Technology and Structural Engineering, University of Aalborg, 1991.
17. Naaman, A. E. & Shah, S. P., Pull-out mechanism in steel fibre-reinforced concrete. *ASCE J. Struct. Div.*, **102**(ST8), (1976) 1537–1548.
18. Balaguru, P. N. & Shah, S. P., *Fiber-Reinforced Cement Composites*. McGraw-Hill, New York, 1992.
19. Tjiptobroto, P. & Hansen, W., Tensile strain hardening and multiple cracking in high-performance cement-based composites containing discontinuous fibers. *ACI Mater. J.*, **90**(1), (1993) 16–25.
20. Banthia, N. & Yan, C., Bond-slip characteristics of steel fibres in high reactivity metakaolin (HRM) modified cement-based matrices. *Cem. Conc. Res.*, **26**(5), (1996) 657–662.
21. Karihaloo, B. L., *Fracture Mechanics and Structural Concrete*. Longman Scientific and Technical, UK, 1995.
22. Stang, H., Li, Z. & Shah, S. P., Pullout problem: stress versus fracture mechanical approach. *J. Eng. Mech.*, **116**(10), (1990) 2136–2150.
23. Hsueh, C.-H., Crack-wake interfacial debonding criteria for fibre-reinforced ceramic composites. *Acta Mater.*, **44**(6), (1996) 2211–2216.
24. Li, V. C., Postcrack scaling relations for fibre reinforced cementitious composites. *J. Mater. Civil Eng.*, **4** 1 (1992) 41–57.
25. Li, V. C., Stang, H. & Krenchel, H., Micromechanics of crack bridging in fibre-reinforced concrete. *Mater. Struct.*, **26** (1993) 486–494.
26. Melin, S., Why do cracks avoid each other?. *Int. J. Fract.*, **13** (1983) 641–654.
27. Nielsen, L. F., Elastic properties of two-phase materials. *Mater. Sci. Eng.*, **52** (1982) 39–62.
28. Nielsen, L. F., Beton og lignende materialers stivhed. Report TR-208. Technical University of Denmark, 1990 (in Danish).
29. Nielsen, L. F., Porøse materialers stivhed. Report TR-287. Technical University of Denmark, 1993 (in Danish).
30. Nielsen, L. F., Stiffness of fibre composites. Report TR-264. Technical University of Denmark, 1992.
31. Li, V. C. & Huang, J., Crack trapping and bridging as toughening mechanisms in high strength concrete. In Proc. Int. Conf. 1990, *Micromechanics of Failure of Quasi-Brittle Materials*, eds S. P. Shah & S. P. Swartz. Elsevier, London, 1990, pp. 579–588.
32. Lange-Kornbak, D. & Karihaloo, B. L., Design of concrete mixes for minimum brittleness. *Adv. Cem. Based Mater.*, **3** (1996) 124–132.
33. Brandt, A. M., *Cement-Based Composites: Materials, Mechanical Properties and Performance*. Spon, London, 1995.
34. Bache, H. H., Concrete and concrete technology in a broad perspective. In Proc. Nordic Symp. 1995, *Modern Design of Concrete Structures*, ed. K. Aakjr. Aalborg University, Denmark, 1995, pp. 1–45.
35. Murakami, Y., *Stress Intensity Factors Handbook*. Pergamon, Oxford, 1988.

APPENDIX A

Bridging stress relationship outside the slip zone

The bridging force carried by a fibre with short embedment length l, oriented at an angle ϕ and stressed $\bar{\delta}$ is $P(\bar{\delta},\phi,l) = \tau\pi dl\, e^{f\phi}$, where the interfacial shear stress $\tau = (\tau_v^*/\bar{\delta}_0)\bar{\delta} = [\tau_v^*/(\zeta\delta_0^s)]\bar{\delta} = \tau_v\bar{\delta}/\delta_0^s$ with $\delta_0^s = 2\tau_g L l/(E_f d)$.

From eqn 1, it follows that the bridging stress is

$$p(\bar{\delta}) = \frac{V_f}{A_f}\,\frac{\tau_v}{\tau_g}\,\frac{d^2}{L^2}\,E_f\pi\bar{\delta}\int_{\phi=0}^{\pi/2}\int_{z=0}^{(L/2-\bar{\delta})\cos\phi} e^{f\phi}\sin\phi\, dz\, d\phi \tag{25}$$

where

$$\int_{z=0}^{(L/2-\bar{\delta})\cos\phi} e^{f\phi}\sin\phi\, dz = e^{f\phi}\sin\phi\,[z]_{z=0}^{(L/2-\bar{\delta})\cos\phi} = \frac{1}{2}\left(\frac{1}{2}L-\bar{\delta}\right)e^{f\phi}\sin 2\phi \tag{26}$$

such that

$$\int_{\phi=0}^{\pi/2}\int_{z=0}^{(L/2-\bar{\delta})\cos\phi} e^{f\phi}\sin\phi\, dz\, d\phi = \frac{1}{2}\left(\frac{1}{2}L-\bar{\delta}\right)\int_{\phi=0}^{\pi/2} e^{f\phi}\sin 2\phi\, d\phi \tag{27}$$

with

$$\int_{\phi=0}^{\pi/2} e^{f\phi}\sin 2\phi\, d\phi = \frac{1}{2}\left(\frac{1}{2}L-\bar{\delta}\right)\left[\frac{e^{f\phi}(f\sin 2\phi - 2\cos 2\phi)}{4+f^2}\right]_{\phi=0}^{\pi/2} = \frac{2}{4+f^2}\left(e^{f\pi/2}+1\right) = h \tag{28}$$

where h is the snubbing factor.

Finally,

$$p(\bar{\delta}) = \frac{V_f}{A_f}\,\frac{\tau_v}{\tau_g}\,\frac{d^2}{L^2}\,E_f\pi\bar{\delta}\,\frac{1}{2}\left(\frac{L}{2}-\bar{\delta}\right)h = 2V_f\,\frac{\tau_v}{\tau_g}\,E_f h\left(\frac{1}{L}\,v_t - \frac{4}{L^2}\,v_t^2\right) \tag{29}$$

since $\bar{\delta} = 2v_t$ and $A_f = d^2\pi/4$.

APPENDIX B

Bridging stress relationship inside the slip zone

In this case, the reduction of the short embedment length is equal to the slip $\bar{\delta}-\bar{\delta}_0$, thereby producing a bridging force $P(\bar{\delta},\phi,l) = \tau_g^*\pi d[l-(\bar{\delta}-\bar{\delta}_0)]\,e^{f\phi}$. With $\tau_g^* = \tau_g\zeta$, $\bar{\delta}_0 = \zeta\delta_0^s = \zeta(2\tau_g Ll)/(E_f d)$ and $l = L/2 - z/\cos\phi$, the force is given by $P(\bar{\delta},\phi,l) = \tau_g\zeta\pi d(\alpha L/2 - \bar{\delta} - \alpha z/\cos\phi)\,e^{f\phi}$, where $\alpha = 1+2\tau_g L\zeta/E_f d$.

Following eqn 1, the bridging stress can be written

$$p(\bar{\delta}) = \frac{V_f}{A_f}\,\tau_g\zeta\,\frac{2}{L}\,\pi d\int_{\phi=0}^{\pi/2}\int_{z=0}^{(L/2-\bar{\delta})\cos\phi}\left(\alpha\frac{L}{2}-\bar{\delta}-\alpha\frac{z}{\cos\phi}\right)e^{f\phi}\sin\phi\,dz\,d\phi$$

where

$$\int_{z=0}^{(L/2-\bar{\delta})\cos\phi}\left(\alpha\frac{L}{2}-\bar{\delta}-\alpha\frac{z}{\cos\phi}\right)e^{f\phi}\sin\phi\,dz = e^{f\phi}\sin\phi\left(\alpha\frac{L}{2}z-\bar{\delta}z-\frac{1}{2}\alpha\frac{1}{\cos\phi}z^2\right)_{z=0}^{(L/2-\bar{\delta})\cos\phi}$$

$$= [-\frac{1}{2}L\bar{\delta}+\frac{1}{2}(2-\alpha)\bar{\delta}^2+\frac{1}{8}L^2\alpha]\,e^{f\phi}\sin\phi\cos\phi \tag{31}$$

such that

$$\int_{\phi=0}^{\pi/2}\int_{z=0}^{(L/2-\bar{\delta})\cos\phi}\left(\alpha\frac{L}{2}-\bar{\delta}-\alpha\frac{z}{\cos\phi}\right)e^{f\phi}\sin\phi\,dz\,d\phi = [-\frac{1}{2}L\bar{\delta}+\frac{1}{2}(2-\alpha)\bar{\delta}^2$$

$$+\frac{1}{8}L^2\alpha]\int_{\phi=0}^{\pi/2}e^{f\phi}\sin\phi\cos\phi\,d\phi = [-\frac{1}{2}L\bar{\delta}+\frac{1}{2}(2-\alpha)\bar{\delta}^2+\frac{1}{8}L^2\alpha]\frac{1}{2}h \tag{32}$$

Finally

$$p(\bar{\delta}) = \frac{V_f}{A_f}\,\tau_g\zeta\,\frac{2}{L}\,\pi d\,\frac{1}{2}\,h[-\frac{1}{2}L\bar{\delta}+\frac{1}{2}(2-\alpha)\bar{\delta}^2+\frac{1}{8}L^2\alpha] = \frac{4V_f}{d}\,\tau_g\zeta\,\frac{1}{L}\,h[-\frac{1}{2}L\bar{\delta}+\frac{1}{2}(2-\alpha)\bar{\delta}^2$$

$$+\frac{1}{8}L^2\alpha] = V_f\tau_g\,\frac{L}{d}\,\frac{1}{2}\,h\zeta\left[-\frac{4}{L}\bar{\delta}+\frac{4}{L^2}(2-\alpha)\bar{\delta}^2+\alpha\right] = V_f\tau_g\,\frac{L}{d}\,\frac{1}{2}\,h\zeta\left[-2\left(\frac{2v_t}{L/2}\right)+(2-\alpha)\left(\frac{2v_t}{L/2}\right)^2+\alpha\right] \tag{33}$$

which is identical to Li's[24] tension softening expression, when $\alpha = 1$, $\zeta = 1$ and $\bar{\delta} = \delta$.

NOMENCLATURE

a	half-length of cracks
a_c	half-length of cracks at the instant of crack coalescence
a_i	half-length of cracks at onset of instability
a_0	half-length of cracks at the attainment of f_t'
A	aspect ratio
A_f	cross-sectional area of a fibre
b	half-length of slip zone
B	brittleness number
d	diameter of fibre
E	modulus of elasticity of fibre composite
E_f	modulus of elasticity of fibre
E_m	modulus of elasticity of the continuous phase in two-phase composite
E_p	modulus of elasticity of the paste
$E(l)$,$E(v_{cr})$	mathematical expectation of l and v_{cr} respectively
$E(z)$,$E(\zeta)$	mathematical expectation of z and ζ respectively
f	snubbing friction coefficient
f_t'	direct tensile strength
$f_{t,a}'$	direct tensile strength of aggregate particle
$f_{t,b}'$	direct tensile strength of composite without fibres
g	maximum aggregate size
g_{av}	average aggregate size
G_F	specific fracture energy
h	snubbing factor $[2/(4+f^2)](e^{f\pi/2}+1)$
K_I	stress intensity factor in mode I
K_{Ic}	critical stress intensity factor in mode I (fracture toughness)
$K_{Ic,p}$	fracture toughness of hardened binder
l	short embedded fibre segment
L	length of a fibre
n	ratio of modulus of elasticity of the discrete phase to that of the continuous phase
$p(z)$	probability density for z
$p(\phi)$	probability density for ϕ
P	force carried by a fibre
P_b	force transmitted by the localization zone due to unbroken matrix ligaments
P_f	force transmitted by the localization zone due to fibres
P_0	force carried by a fibre at the attainment of fully developed slip
u	total half-opening of crack where slip is assumed to initiate
v_{cr}	local half-opening of crack in single-fibre pull-out at onset of slip
$\bar{v}_{cr}$	effective half-opening of crack where slip initiates
v_t	local half-opening of crack
V	volume fraction of the discrete phase in two-phase composite
V_c	volume fraction of cement particles
V_f	volume fraction of fibre
V_{ms}	volume fraction of microsilica particles
V_p	volume fraction of paste
V_w	volume fraction of water and dispersing agent
w	inelastic deformation of the localization zone
w_k	inelastic deformation of the localization zone at the instant of crack coalescence
w_t	total deformation of the localization zone
w/c	water/cement ratio
W	crack spacing in the localization zone
z	distance from the centroid of the fibre to the crack plane

Greek letters

α	factor $1+[2\tau_g LE(\zeta)]/(E_f d)$
β	constant
χ	crack trapping parameter
δ	mouth opening of crack in multiple-fibre pull-out test
$\bar{\delta}$	effective opening of crack in multiple-fibre pull-out test
δ_0	mouth opening of crack in multiple-fibre pull-out test at onset of fully developed slip
$\bar{\delta}_0$	effective opening of crack in multiple-fibre pull-out test at onset of fully developed slip
δ_0^s	mouth opening of crack in single-fibre pull-out test at onset of fully developed slip
$\bar{\delta}_0^s$	effective opening of crack in single-fibre pull-out test at onset of fully developed slip
δ^s	mouth opening of crack in single-fibre pull-out test
$\bar{\delta}^s$	effective opening of crack in single-fibre pull-out test

η toughening ratio
γ constant
ϕ orientation angle of a fibre to a plane perpendicular to the crack
ρ_c density of unhydrated cement particles
ρ_w density of water
σ tensile stress
τ fibre–matrix interfacial shear stress
τ_g shear stress at fibre–matrix interface during pull-out of single fibre
τ_g^* shear stress at fibre–matrix interface during multiple-fibre pull-out
τ_v maximum attainable shear stress at fibre–matrix interface in single-fibre pull-out test
τ_v^* maximum attainable shear stress at fibre–matrix interface in multiple-fibre pull-out test
Θ geometry function accounting for the configuration of the discrete phase
φ orientation angle of a fibre to the loading direction
ζ ratio $\bar{\delta}_0/\delta_0^s = \bar{v}_{cr}/v_{cr}$